

*ARMY RESEARCH LABORATORY*



**U.S. Army Research Laboratory (ARL) Nuclear Magnetic  
Resonance Based Spectroscopic Analysis via Magnetic  
Resonance Force Microscopy**

**by Dimitri Alexson and Doran D. Smith**

**ARL-TR-6119**

**August 2012**

## **NOTICES**

### **Disclaimers**

The findings in this report are not to be construed as an official Department of the Army position unless so designated by other authorized documents.

Citation of manufacturer's or trade names does not constitute an official endorsement or approval of the use thereof.

Destroy this report when it is no longer needed. Do not return it to the originator.

# **Army Research Laboratory**

Adelphi, MD 20783-1197

---

**ARL-TR-6119****August 2012**

---

## **U.S. Army Research Laboratory (ARL) Nuclear Magnetic Resonance Based Spectroscopic Analysis via Magnetic Resonance Force Microscopy**

**Dimitri Alexson and Doran D. Smith**  
**Sensors and Electron Devices Directorate, ARL**

| REPORT DOCUMENTATION PAGE   |                             |                              |  | Form Approved<br>OMB No. 0704-0188                         |   |
|---|-----------------------------|------------------------------|--|--|---|
| <p>Public reporting burden for this collection of information is estimated to average 1 hour per response, including the time for reviewing instructions, searching existing data sources, gathering and maintaining the data needed, and completing and reviewing the collection information. Send comments regarding this burden estimate or any other aspect of this collection of information, including suggestions for reducing the burden, to Department of Defense, Washington Headquarters Services, Directorate for Information Operations and Reports (0704-0188), 1215 Jefferson Davis Highway, Suite 1204, Arlington, VA 22202-4302. Respondents should be aware that notwithstanding any other provision of law, no person shall be subject to any penalty for failing to comply with a collection of information if it does not display a currently valid OMB control number.</p> <p><b>PLEASE DO NOT RETURN YOUR FORM TO THE ABOVE ADDRESS.</b></p> |                             |                              |  |  |   |
| 1. REPORT DATE (DD-MM-YYYY)<br>August 2012  |                             | 2. REPORT TYPE<br>Final      |  | 3. DATES COVERED (From - To)<br>FY11                       |   |
| 4. TITLE AND SUBTITLE<br>U.S. Army Research Laboratory (ARL) Nuclear Magnetic Resonance Based Spectroscopic Analysis via Magnetic Resonance Force Microscopy  |                             |                              |  | 5a. CONTRACT NUMBER  |   |
|   |                             |                              |  | 5b. GRANT NUMBER   |   |
|   |                             |                              |  | 5c. PROGRAM ELEMENT NUMBER                                 |   |
| 6. AUTHOR(S)<br>Dimitri Alexson and Doran D. Smith  |                             |                              |  | 5d. PROJECT NUMBER<br>DE-EM000358                          |   |
|   |                             |                              |  | 5e. TASK NUMBER  |   |
|   |                             |                              |  | 5f. WORK UNIT NUMBER                                       |   |
| 7. PERFORMING ORGANIZATION NAME(S) AND ADDRESS(ES)<br>U.S. Army Research Laboratory<br>ATTN: RDRL-SEE-O<br>2800 Powder Mill Road<br>Adelphi MD 20783-1197   |                             |                              |  | 8. PERFORMING ORGANIZATION<br>REPORT NUMBER<br>ARL-TR-6119 |   |
| 9. SPONSORING/MONITORING AGENCY NAME(S) AND ADDRESS(ES)   |                             |                              |  | 10. SPONSOR/MONITOR'S ACRONYM(S)                           |   |
|   |                             |                              |  | 11. SPONSOR/MONITOR'S REPORT<br>NUMBER(S)                  |   |
| 12. DISTRIBUTION/AVAILABILITY STATEMENT<br>Approved for public release; distribution unlimited.   |                             |                              |  |  |   |
| 13. SUPPLEMENTARY NOTES   |                             |                              |  |  |   |
| 14. ABSTRACT<br>The overall goal of this program is to develop magnetic resonance force microscopy (MRFM) based methods for the spectroscopic identification and characterization of Department of Energy (DOE) supplied samples. Work is currently divided among three participants: (1) Department of Energy (DOE) laboratories at Savannah River National Laboratory (SRNL) and Oak Ridge National Laboratory (ORNL), (2) the U.S. Army Research Laboratory (ARL), and (3) U.S. Naval Research Laboratory (NRL). This report summarizes only the work done at ARL during fiscal year 2011 (FY11).  |                             |                              |  |  |   |
| 15. SUBJECT TERMS<br>Magnetic resonance force microscopy, NMR, spectroscopy   |                             |                              |  |  |   |
| 16. SECURITY CLASSIFICATION OF:   |                             |                              | 17. LIMITATION<br>OF<br>ABSTRACT<br>UU | 18. NUMBER<br>OF<br>PAGES<br>22                            | 19a. NAME OF RESPONSIBLE PERSON<br>Dimitri Alexson          |
| a. REPORT<br>Unclassified   | b. ABSTRACT<br>Unclassified | c. THIS PAGE<br>Unclassified |  |  | 19b. TELEPHONE NUMBER (Include area code)<br>(301) 394-2523 |

---

## Contents

---

|  |           |
|--|-----------|
| <b>List of Figures</b>   | <b>iv</b> |
| <b>1. Technical Objectives</b>   | <b>1</b>  |
| <b>2. Technical Approach</b>   | <b>1</b>  |
| <b>3. Progress Statement Summary</b>   | <b>1</b>  |
| <b>4. Background</b>   | <b>2</b>  |
| <b>5. Progress</b>   | <b>7</b>  |
| 5.1 Spectroscopy of the Bulk and Image Slice Regions.....                                      | 7         |
| 5.2 Inversion-recovery Technique.....  | 9         |
| 5.3 Sample Shuttling Constraints .....   | 10        |
| 5.4 RF Nutation .....  | 10        |
| <b>6. Organizational and Related Meetings</b>  | <b>11</b> |
| <b>7. Future Work</b>  | <b>11</b> |
| 7.1 Increase the Magnitude of $B_1$ .....  | 11        |
| 7.2 Perform NMR Spectroscopy on the DOE Sample of Interest Using MRFM .....                    | 11        |
| 7.3 Determine the Limitations of MRFM Spectroscopy .....                                       | 12        |
| 7.4 Coordinate with Conventional NMR Spectroscopy .....  | 12        |
| 7.5 Install Interferometers on All Three Axis of the Sample Stage So Indexing is Possible..... | 12        |
| <b>8. Final Summary and Signature Conclusion</b>   | <b>12</b> |
| <b>9. References</b>   | <b>13</b> |
| <b>List of Symbols, Abbreviations, and Acronyms</b>  | <b>14</b> |
| <b>Distribution List</b>   | <b>15</b> |

---

## List of Figures

---

|  |    |
|--|----|
| Figure 1. Force detected MRFM. $B_0$ is the background magnetic field, $m$ is the particle's magnetic moment, and $\mu$ is the sample's magnetic moment. The cantilever is driven back and forth as the RF magnetic field generated by the RF coil oscillates the sample's magnetic moment. ....   | 3  |
| Figure 2. Nano-MRI. The magnetic particle creates a rapidly changing magnetic field across the sample. Using the techniques of NMR, it is possible to reverse the spins only in a sensitive slice. ....  | 4  |
| Figure 3. The CERMITE MRFM technique. $B_0$ is the static magnetic field, $m$ is the particle's magnetic moment, and RF is the direction of the RF magnetic field generated by the RF coil (not shown). The cantilever is driven to a constant oscillation amplitude (in and out of the paper), the spins in the resonant shell (shown in red) are reversed by an RF pulse, and the signal is registered as a change in the cantilever's resonance frequency. .... | 4  |
| Figure 4. Photograph of the apparatus used to collect data described in this report. The top surface of the GaAs sample is gold coated. The reflection of the 5- $\mu\text{m}$ nickel (Ni) sphere, cantilever, and optical fiber are seen in the gold. ....  | 5  |
| Figure 5. Two different regions near the magnetic particle where spectroscopy was performed: the bulk region and the image slices. Note that at the magic angle the $z$ component of the particle's magnetic field is zero; it points only in the $xy$ -plane. The image slices offer higher resolution; the bulk region offers a higher signal-to-noise ratio (SNR). ....   | 6  |
| Figure 6. The signal displayed here was obtained by performing several overlapping CERMITE scans. ....   | 7  |
| Figure 7. Typical FIDs of GaAs at 5 K and 5 T. ....  | 8  |
| Figure 8. FT of typical FID data, from the slice region of the sample. The slice region in MRFM of the sample results in the highest spatial resolution. The spectrum shown here is the result of a complex FT of the orthogonal $\{xx\}$ and $\{xy\}$ FID curves, which uniquely identifies the sign of the chemical shift. This is standard practice in NMR spectroscopy. ....   | 9  |
| Figure 9. GaAs $T_1$ vs. temperature. ....   | 10 |

---

## **1. Technical Objectives**

---

The development of magnetic resonance force microscopy (MRFM) techniques and spectroscopic protocols to examine the physical properties of novel materials is the goal of the research at the U.S. Army Research Laboratory (ARL). A specific objective is to analyze a well-characterized gallium arsenide (GaAs) crystal to show that the instrumentation is capable of performing spectroscopy.

---

## **2. Technical Approach**

---

To accomplish these tasks, ARL fully qualified its MRFM system as capable of performing shuttling based spectroscopy by doing the following:

1. Modifying the current MRFM instrumentation to enable the spectroscopic investigation of novel materials.
  2. Authoring all the needed support software.
  3. Comparing a model to experimental data
- 

## **3. Progress Statement Summary**

---

During fiscal year 2011 (FY11), the primary accomplishments were the following:

- Demonstrated nuclear magnetic resonance (NMR) spectroscopy on GaAs.
- Demonstrated measurement of  $T_1$  versus temperature using a real-time inversion-recovery technique.
- Determined the source of the extra frequency noise in the driven cantilever.
- Authored programs to control automated shuttling, allows data collection for 72 h without user intervention.
- Authored programs to measure value of radio frequency (RF) magnetic field.
- Added an optical interferometer to measure the shuttling distance.
- Demonstrated a shuttling resolution of  $\pm 10$  nm.

- Modeled high resolution cantilever enhanced resonance of magnetization inversion transients (CERMIT) lineshape with Mathematica.
  - Designed and purchased most of the components for a dual wavelength interferometer on all three axes of the sample stage and the cantilever.
- 

## 4. Background

---

MRFM combines two technologies: (1) force microscopy and (2) magnetic resonance (1). The force referred to in the first technology is the force between two magnets. The first magnet is a magnetic particle attached to the end of a soft cantilever (figure 1). The second magnet refers to the sample's magnetic moment, arising from either the nuclei or electrons in the sample. The sample and cantilever system is immersed in a large static magnetic field of several Tesla, which acts to align the sample magnetic moments in parallel to the static magnetic field, while also magnetizing the magnetic particle located on the cantilever. The attraction between the magnetic moments in the sample to the magnetic particle on the cantilever acts to bend the cantilever toward the sample. This displacement of the cantilever is typically measured with a fiber-based optical interferometer capable of picometer displacement sensitivity. The second technology used to make MRFM possible is magnetic resonance. Using the techniques of magnetic resonance, a RF pulse sequence is applied to the sample. This RF pulse acts to rotate the sample's magnetic moment and, depending on the pulse length, it is possible to reverse the direction of the magnetic moments in the sample. As the magnetic moments in the sample are rotated (as a result of the RF pulse), the magnitude of the force on the cantilever also changes, to the point where a total reversal of the magnetic moments in the sample will result in the cantilever being repelled from the sample. By applying an RF pulse periodically, an alternating force is applied to the cantilever, causing the cantilever to oscillate (figure 1). Then, by measuring the amplitude of the cantilever displacement the number of magnetic moments (called spins) being interrogated is determined, i.e., the signal observed is proportional to a force, which is registered as the amplitude of a cantilever oscillation.



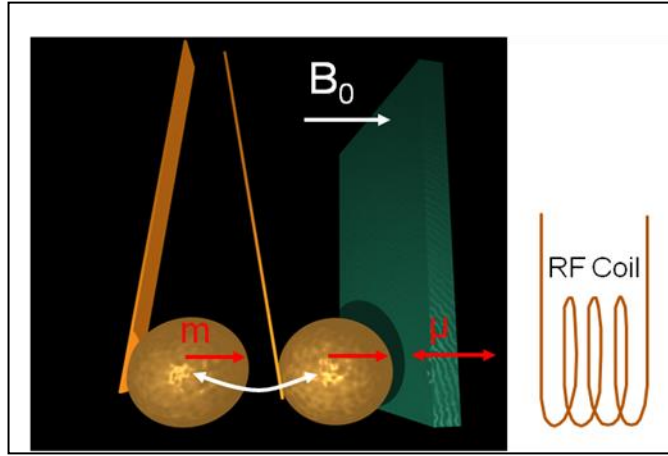


Figure 1. Force detected MRFM.  $B_0$  is the background magnetic field,  $m$  is the particle's magnetic moment, and  $\mu$  is the sample's magnetic moment. The cantilever is driven back and forth as the RF magnetic field generated by the RF coil oscillates the sample's magnetic moment.

By combining force microscopy (technology 1) with magnetic resonance (technology 2), it is possible to directly observe the nuclear magnetic moments in the sample. Further increases in sensitivity are possible. By oscillating the cantilever at its resonant frequency, a  $Q$  enhancement of the cantilever amplitude is obtained.  $Q$  is the quality factor of the cantilever and can easily be 100,000 for a pure silicon (Si) cantilever, demonstrating that it is possible to achieve five orders of magnitude increased sensitivity by operating at the cantilever's resonant frequency.

Using MRFM, it is possible to perform magnetic resonance imaging (MRI) at the nanoscale, i.e., nano-MRI. The rapid decrease in the cantilever-mounted particle's magnetic field, measured as a function of distance from that magnetic particle, results in a magnetic field gradient across the sample (figure 2). Because the *frequency* of the RF pulse must be commensurate with the *total magnetic field* (static background field  $B_0$  plus the magnetic field from the particle on the cantilever) experienced by the sample nuclear magnetic moment (spin), it is possible to select the spatial slice through the sample where spins are reversed. The selected spatial slice is called the sensitive slice in the sample (figure 2). The sensitive slice is a bowl-shaped shell. By moving the sample and magnetic particle in three-dimensions with respect to each other, it is possible to construct a three-dimensional (3-D) image of the sample's spin (magnetic moment) density, hence nano-MRI is achieved.

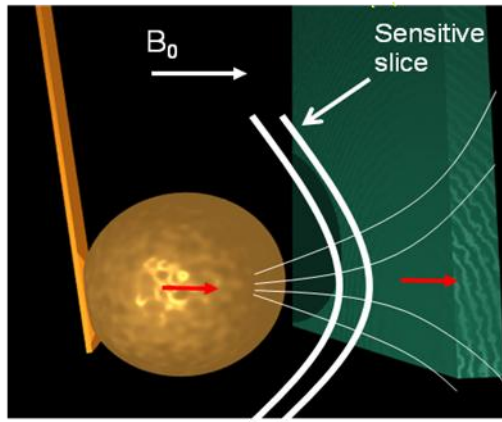


Figure 2. Nano-MRI. The magnetic particle creates a rapidly changing magnetic field across the sample. Using the techniques of NMR, it is possible to reverse the spins only in a sensitive slice.

The MRFM technique used to collect all the data described in this report is CERMIT. CERMIT registers the signal from the cantilever as a change in the cantilever's resonant frequency instead of its amplitude. CERMIT is performed by driving a cantilever, with a magnetic particle glued on its end in this setup, at the cantilever's natural resonance frequency (figure 3). A RF sweep is used to invert the spins in a sensitive slice. The inversion of the spins causes a small (few mHz out of 1000 Hz) shift in the resonant frequency of the driven cantilever that is proportional to the number of spins in the sensitive slice. The signal is measured through a force gradient (2) and is registered as a change in the natural resonance frequency of the driven cantilever.

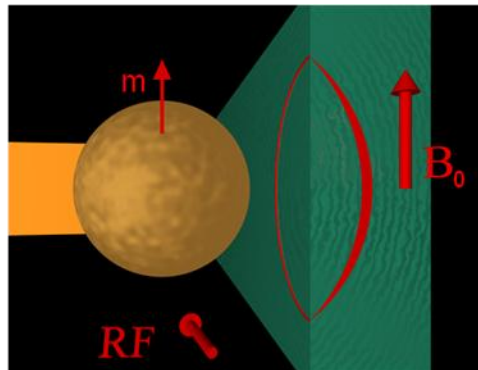


Figure 3. The CERMIT MRFM technique.  $B_0$  is the static magnetic field,  $m$  is the particle's magnetic moment, and RF is the direction of the RF magnetic field generated by the RF coil (not shown). The cantilever is driven to a constant oscillation amplitude (in and out of the paper), the spins in the resonant shell (shown in red) are reversed by an RF pulse, and the signal is registered as a change in the cantilever's resonance frequency.

Figure 4 is a photograph of the principal components used to acquire the data described in this report.

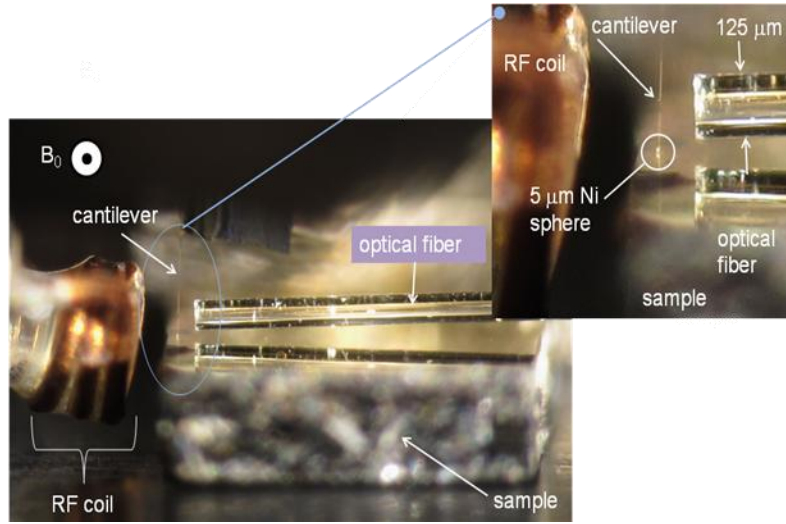


Figure 4. Photograph of the apparatus used to collect data described in this report. The top surface of the GaAs sample is gold coated. The reflection of the 5- $\mu\text{m}$  nickel (Ni) sphere, cantilever, and optical fiber are seen in the gold.

Although the goal of this work is to perform NMR-based spectroscopy using MRFM, there is an apparent contradiction in the method being employed. Conventional electrically detected NMR-based spectroscopy relies on very homogeneous magnetic fields. Fields can be as uniform as 1 part in  $10^{11}$ . MRFM, on the other hand, uses very inhomogeneous magnetic fields (1 part in 25), which arise from the magnetic particle located on the cantilever tip. This contradiction is resolved by temporarily removing the magnetic field inhomogeneity from the sample (3, 4). This is accomplished by shuttling (moving) the sample away from the cantilever until the magnetic field is uniform enough to apply typical NMR techniques. Since the magnetic field inhomogeneity from the magnetic particle on the cantilever falls off as  $(a/r)^4$ , where  $a$  is the particle radius and  $r$  is the distance from the particle center, large shuttling distances are not required (just 10's of micrometers for this work) to establish a homogenous magnetic field. After the cantilever with the magnetic particle is shuttled away from the sample and a homogenous magnetic field is restored, conventional NMR techniques are applied. The sample is then shuttled back towards the cantilever and the MRFM signal is read out using the CERMIT technique.

Using the shuttling technique, NMR-based spectroscopy with MRFM approximately 1000 times more sensitive than any previous work (4) has been demonstrated. Figure 5 shows the magnetic particle (normally attached to the cantilever) and the different regions in which we have performed spectroscopy. The lines shown are the magnetic field lines due to a magnetic dipole (sphere). The magnetic field lines leave the top half of the particle pointing perpendicular to the surface of the sphere (in the  $+z$ -direction), bend around to point in the  $x$ -direction, continue to

bend even more such that the magnetic field line points down ( $-z$ ) and eventually reenters the bottom half of the particle pointing in the  $+z$ -direction again. The line (a cone in a 3-D world) at which the particle's magnetic field lines have no  $z$ -component is called the magic angle and occurs at  $\pm 54.74^\circ$ . The magic angle divides the sample into three separate regions: the bulk, magic angle, and image slice regions. The bulk region is the largest and occupies the area outside of the magic angle. In the bulk region, the  $z$ -component of the particle's magnetic field is parallel to  $B_0$  (points in the  $+z$ -direction). The part of the bulk region that yields a spectroscopy signal extends many particle diameters away from the particle. At the magic angle, the particle's  $z$ -component of the magnetic field is zero. As the magnetic field crosses from the bulk region to the image slice region, the  $z$ -component goes from being parallel ( $+z$ ) to antiparallel ( $-z$ ) with respect to  $B_0$ . The region inside the magic angle is called the image slice region. In this region, the particle's magnetic field is antiparallel ( $-z$ ) to  $B_0$ . It is here where the highest resolution slices are found and is the region usually associated with MRFM's high resolution ability.

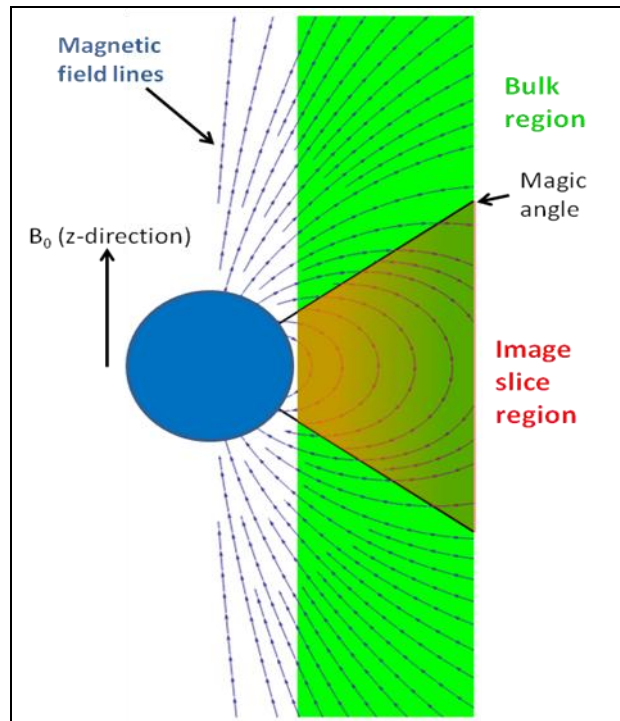


Figure 5. Two different regions near the magnetic particle where spectroscopy was performed: the bulk region and the image slices. Note that at the magic angle the  $z$  component of the particle's magnetic field is zero; it points only in the  $xy$ -plane. The image slices offer higher resolution; the bulk region offers a higher signal-to-noise ratio (SNR).

The total magnetic field (of interest to the MRFM experiment) experienced by the sample is the sum of  $B_0$  and the particle's magnetic field. Because  $B_0$  is of the order of 5 T and the magnetic particle's field is of the order of 0.2 T, the total magnetic field always points predominately in

the  $+z$ -direction. The particle's magnetic field either adds or subtracts small amounts of field from  $B_0$ . This changing total magnetic field experienced by the sample in the region of the magnetic particle enables us to perform spectroscopy in different regions as described in section 5.

## 5. Progress

### 5.1 Spectroscopy of the Bulk and Image Slice Regions

Figure 6 shows the MRFM signal obtained with the CERMIT protocol from each of the three regions. The MRFM signal is proportional to the number of spins in each region. The image slice region (data at the far left of the plot) is obtained from the slices closest to and directly under the magnetic particle connected to the cantilever. Data points closer to the magic angle peak are from image slices that extend deeper into the sample. The data points at the magic angle peak are obtained from a thin shell surrounding the magic angle. Data points in the bulk region close to the magic angle are slices that are closer to the magic angle. Data points to the far right of the plot are from slices more remote from the magic angle. We have performed spectroscopy on spins in the bulk region and in the image slice region. The results are described in section 5.2.

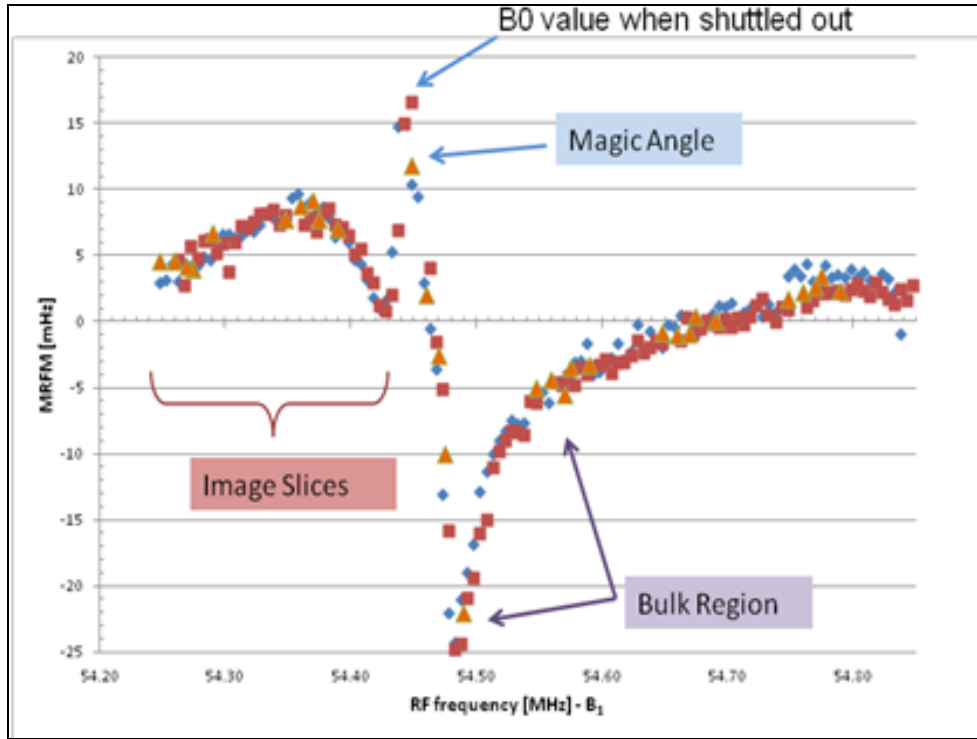


Figure 6. The signal displayed here was obtained by performing several overlapping CERMIT scans.

NMR spectroscopy was demonstrated on the bulk and slice spatial regions of GaAs at 5 K and a  $B_0$  value of 5 T. The magnetic particle located on the cantilever was approximately 5  $\mu\text{m}$  in diameter. The sample to magnetic particle distance was 300 nm when the CERMIT protocol was used to read out the NMR-based spectroscopy signal. In order to remove the magnetic field inhomogeneities due to the magnetic particle, the sample was shuttled out to a distance of 65  $\mu\text{m}$ . While shuttled out, the NMR RF spectroscopic pulse sequence was delivered. The RF pulse,  $B_1$ , was at a frequency of 50 MHz and had a magnitude of 0.75 mT. The first RF pulse sequence used consisted of two pulses separated by a variable time delay and a relative phase shift between the two pulses of  $0^\circ$  (an  $xx$ -pulse). The frequency of  $B_1$  was also varied. The free induction decay (FID) plots for three  $B_1$  frequencies are shown in figure 7.

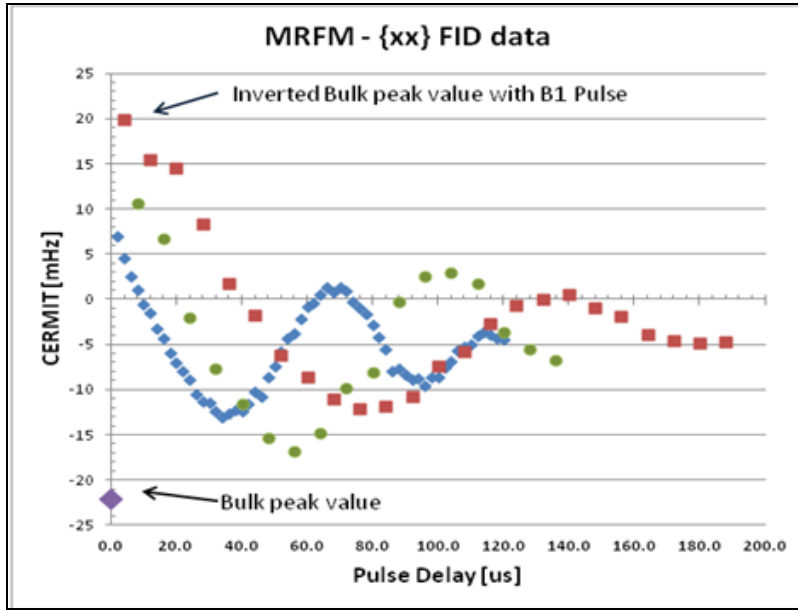


Figure 7. Typical FIDs of GaAs at 5 K and 5 T.

The FID contains the NMR spectroscopic information about the sample that allows us to distinguish one compound from another. When an RF pulse is applied to a spin system that is initially aligned parallel to  $B_0$  (the  $+z$ -axis direction), the spins rotate away from the  $z$ -axis toward the  $xy$ -plane. The RF pulse is timed to turn off just as the spins get to the  $xy$ -plane. The spins then rotate in the  $xy$ -plane about the  $z$ -axis at approximately 50 MHz. During the time, the nuclear spins spend in the  $xy$ -plane, some of those spins will re-equilibrate along the  $+z$ -axis, while others will fan out in the  $xy$ -plane. Both of these interactions (termed relaxation) act to reduce the total number of spins that it is possible to observe. The longer the holding time is in the  $xy$ -plane, the fewer spins it is possible to recover for interrogation. Therefore, after a predefined time (2–200  $\mu\text{s}$ ), a second RF pulse is applied to the spins, causing them to rotate from the  $xy$ -plane back along the  $+z$ -axis. After the application of the second pulse, the sample is shuttled back in to read out the magnitude of the  $z$ -component, which is left after the relaxation phenomenon has occurred. Figure 7 shows three FID plots where the pulse delay between the

first and second RF pulses is plotted on the  $x$ -axis with the magnitude of the signal plotted on the  $y$ -axis. The resulting signal, when plotted as a function of the pulse delay, is a decaying sine wave. The frequency of the sine wave reports on the spin's  $xy$ -plane rotation speed, i.e., 50.000 or 50.001 MHz. The rate the sine wave decays reports on the amount of spins that survived their precession in the  $xy$ -plane. Both of these facts provide significant clues to the spin's local chemical environment.

A typical Fourier transform (FT) of the FIDs in figure 7 is shown in figure 8. The offset of the peak center from 0 Hz allows us to determine the spin's exact precession frequency while in the  $xy$ -plane. The linewidth of typically 8–10 kHz tells us that the  $^{69}\text{Ga}$  nuclei are in a crystal lattice that is moderately strained. If the GaAs crystal lattice were unstrained, the linewidth would be 3 kHz. It is also possible that a hole burning experiment is being done and that  $B_1$  is not sampling the total spectrum. This may be why the period of the FID curve decreases as the frequency of  $B_1$  is moved off resonance (figure 7). Planned increases in the magnitude of  $B_1$  will allow for harder pulses, which should capture the entire spectrum at once.

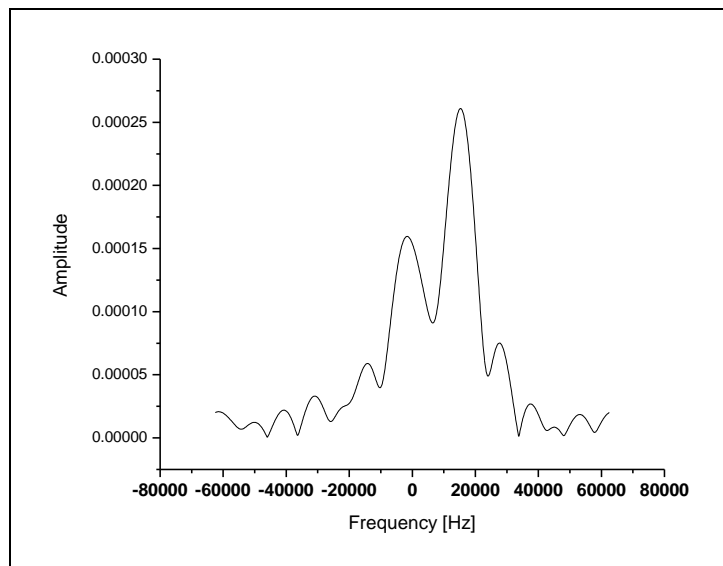


Figure 8. FT of typical FID data, from the slice region of the sample. The slice region in MRFM of the sample results in the highest spatial resolution. The spectrum shown here is the result of a complex FT of the orthogonal  $\{xx\}$  and  $\{xy\}$  FID curves, which uniquely identifies the sign of the chemical shift. This is standard practice in NMR spectroscopy.

## 5.2 Inversion-recovery Technique

Another common technique in magnetic resonance is the measurement of the spin-lattice relaxation,  $T_1$ , with an inversion recovery experiment. In contrast to modern electrically detected NMR instruments, which are only sensitive to the transverse magnetization, MRFM can capture the entire saturation recovery curve in one experiment lasting a time the order of  $T_1$ . A single adiabatic rapid passage (ARP) is used to sweep through resonance that inverts the initial



polarization. In the case of  $^{69}\text{Ga}$  nuclei, which experience quadrupolar interaction,  $T_1$  was measured from 4 to 25 K and does not remain constant as a function of temperature (figure 9).

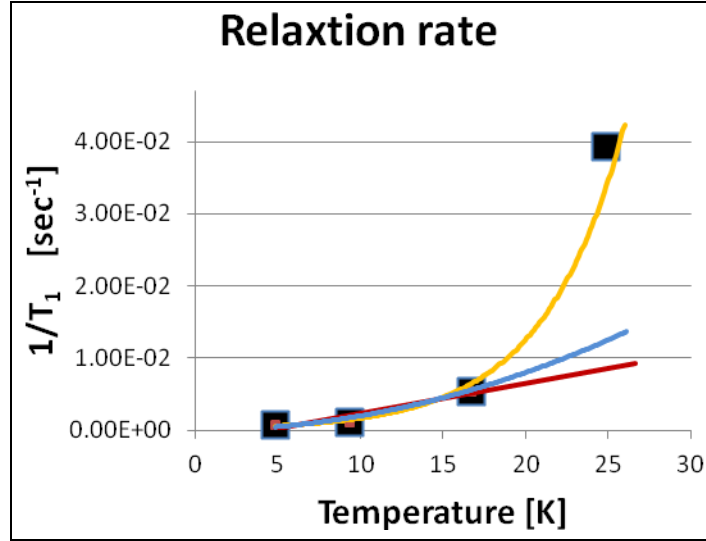


Figure 9. GaAs  $T_1$  vs. temperature.

### 5.3 Sample Shuttling Constraints

Recall that the sample is shuttled out to reduce the particle's magnetic field inhomogeneity across the sample to some desired level. The desired level is the level at which the inhomogeneity is smaller than the desired spectroscopic resolution (linewidth).

Another constraint of this protocol results from the requirement that once the NMR RF spectroscopic sequence is applied, the sample must be shuttled back to the cantilever to read out the data in a time less than  $T_1$ . The GaAs sample has a  $T_1$  of 20 min and the sample shuttle-in time used was 45 s. The Department of Energy (DOE) sample's  $T_1$  of 25 s require that a sample shuttle-in time of 3–5 s be used. This is the current systems demonstrated minimum shuttle time.

### 5.4 RF Nutation

To perform NMR-based spectroscopy, RF pulses of known length, phase, and magnetic field strength  $|B_1|$  are delivered to the sample. An arbitrary waveform generator determines the pulse length and phase to high precision. The length of the pulse needed to rotate spins that are initially parallel to the  $z$ -axis into the  $xy$ -plane, referred to as a  $\pi/2$  pulse, is determined by the magnitude of  $B_1$ . A RF nutation experiment is done in order to calibrate the magnitude of  $B_1$  versus RF power and thus determine the length of a  $\pi/2$  pulse. Due to the geometry of the RF coil with respect to the sample, the spins being interrogated in the sample are 20  $\mu\text{m}$  further from the face of the coil when shuttled. For  $B_1$  calibration, the sample is shuttled to the same distance that will be used for spectroscopy, thus maintaining the calibration.



When a RF pulse is applied to a spin system that is initially polarized along the +z-axis (parallel to  $+B_0$ ), the spin system polarization rotates away from the z-axis so that the direction of the polarization forms an angle  $\theta$  with respect to the z-axis. The angle  $\theta$  is a function of both the length of the pulse and the magnitude of  $B_1$ . To measure the magnitude of  $B_1$  a series of RF pulses with constant phase and constant magnitude (RF power) but with varying lengths are used. The resulting MRFM signal, when plotted as a function of the pulse length, is a decaying sine wave. The duration of a  $\pi/2$  pulse is thus determined by one quarter of the sine wave period. For the case of GaAs spectroscopy work,  $B_1$  was determined to be 0.75 mT for 7 W of RF power. This results in a  $\pi/2$  pulse length of 32.5  $\mu$ s.

---

## **6. Organizational and Related Meetings**

---

An FY11 kickoff meeting was held at Oak Ridge National Laboratory (ORNL) in November 2011. At the meeting, there were representatives from ORNL, Savannah River National Laboratory (SRNL), U.S. Naval Research Laboratory (NRL), ARL, and Lawrence Livermore National Laboratory (LLNL). Two days worth of discussions were held during which the accomplishments for FY10 were discussed and plans for FY11 were made.

In March 2011, a meeting was held in Washington, DC, with the program manager Les Pitts. Presentations were given by representatives from ORNL, SRNL, NRL and ARL.

In June 2011, ARL hosted a Schubert Review of the project. Presentations were given by representatives from ORNL, SRNL, NRL and ARL. The feedback from the review panel was very positive.

---

## **7. Future Work**

---

### **7.1 Increase the Magnitude of $B_1$**

It became apparent during FY11 that the magnitude of  $B_1$ , 0.75 mT when using 7 W of RF power is not sufficient to invert the entire width of the spectroscopic line. Therefore, modifications are underway, starting in October 2011, to upgrade the MRFM probe's RF circuitry. The planned modifications will reduce the heat generated in the cryogenic portion of the probe and allow for higher RF powers, resulting in a larger  $B_1$ .

### **7.2 Perform NMR Spectroscopy on the DOE Sample of Interest Using MRFM**

As soon as the RF modifications are complete, we will begin performing spectroscopy on DOE samples of interest.

### **7.3 Determine the Limitations of MRFM Spectroscopy**

Since MRFM cannot use magic angle spinning (MAS), its ability to distinguish between different compounds with similar spectroscopy is limited. The study will involve determining if it is possible to distinguish between all the related compounds that are likely to be encountered.

### **7.4 Coordinate with Conventional NMR Spectroscopy**

A vital part of this research is our collaboration with Dr. Chris Klug of NRL. Dr. Klug is a solids NMR expert. He is leading the effort in determining protocols to distinguish between different compounds in a non-MAS environment. Our continued collaboration is critical to the success of this project.

### **7.5 Install Interferometers on All Three Axis of the Sample Stage So Indexing is Possible**

For some of the DOE samples, it is necessary for MRFM to perform spectroscopy at specific locations on the sample. By installing dual wavelength interferometers on all three axes of the sample stage, it will be possible to find predefined locations on the sample surface.

---

## **8. Final Summary and Signature Conclusion**

---

During FY11, ARL demonstrated shuttling-based NMR spectroscopy with MRFM with a GaAs crystal at 5 K and 5 T on sample volume 1000 times smaller than any previous work on any sample. This milestone, coupled with the NRL result that the  $T_1$  of the DOE sample of interest is 25 s, are the two enabling demonstrations that allow us to claim NMR spectroscopy on DOE's samples of interest with MRFM will be possible in FY12.

---

## 9. References

---

1. Sidles, J. A. Noninductive Detection of Single-proton Magnetic Resonance. *Applied Physics Letters* **1991**, 58 (24), 2854–2856.
2. Garner, Sean, R., et al. Force-gradient Detected Nuclear Magnetic Resonance. *Appl. Phys. Lett.* **2004**, 84 (25), 5091.
3. Marohn J. A. A Microscale Nuclear Magnetic Resonance Spectrometer for Remote Environments, a Research Proposition in Partial Fulfillment of the Requirements for the Degree of Doctor of Philosophy; California Institute of Technology, 1996.
4. Eberhardt, K. W., et al. One- and Two-dimensional NMR Spectroscopy with a Magnetic Resonance Force Microscope. *Angew. Chem. Int.* **2008**, 47, 8961.

---

## List of Symbols, Abbreviations, and Acronyms

---

|        |   |
|--------|---|
| 3-D    | three-dimensional   |
| ARL    | U.S. Army Research Laboratory                                       |
| ARP    | adiabatic rapid passage   |
| CERMIT | cantilever enhanced resonance of magnetization inversion transients |
| DOE    | Department of Energy  |
| FID    | free induction decay  |
| FT     | Fourier transform   |
| FY     | fiscal year   |
| GaAs   | gallium arsenide  |
| LLNL   | Lawrence Livermore National Laboratory                              |
| MAS    | magic angle spinning  |
| MRFM   | magnetic resonance force microscopy                                 |
| MRI    | magnetic resonance imaging  |
| Ni     | nickel  |
| NMR    | nuclear magnetic resonance  |
| NRL    | U.S. Naval Research Laboratory                                      |
| ORNL   | Oak Ridge National Laboratory                                       |
| RF     | radio frequency   |
| Si     | silicon   |
| SNR    | signal-to-noise ratio   |
| SRNL   | Savannah River National Laboratory                                  |

1  
ELEC      ADMNSTR  
         DEFNS TECHL INFO CTR  
         ATTN DTIC OCP  
         8725 JOHN J KINGMAN RD STE 0944  
         FT BELVOIR VA 22060-6218

7           US ARMY RSRCH LAB  
         ATTN IMAL HRA MAIL & RECORDS MGMT  
         ATTN RDRL CIO LL TECHL LIB  
         ATTN RDRL CIO LT TECHL PUB  
         ATTN RDRL SEE I P UPPAL  
         ATTN RDRL SEE O D ALEXSON  
         ATTN RDRL SEE O D SMITH  
         ATTN RDRL SEE O M MONTI  
         ADELPHI MD 20783-1197

INTENTIONALLY LEFT BLANK.